Research Article

NEURAL REGENERATION RESEARCH
www.nrronline.org

Empowering the NSC-34 cell line as a motor neuron model: cytosine arabinoside's action

Giuseppe Vitale[1, †], Susanna Amadio[1], Francesco Liguori[1, 2], Cinzia Volonté[1, 2, *]

https://doi.org/10.4103/NRR.NRR-D-24-00034

Date of submission: January 9, 2024

Date of decision: July 31, 2024

Date of acceptance: August 30, 2024

Date of web publication: September 24, 2024

From the Contents

Graphical Abstract

Long-lasting and homogeneous differentiation of motor neuron NSC-34 cells by cytosine arabinoside

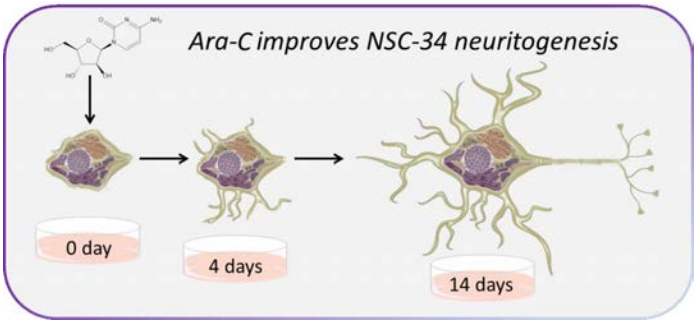

Abstract

The NSC-34 cell line is a widely recognized motor neuron model and various neuronal differentiation protocols have been exploited. Under previously reported experimental conditions, only part of the cells resemble differentiated neurons; however, they do not exhibit extensive and time-prolonged neuritogenesis, and maintain their duplication capacity in culture. The aim of the present work was to facilitate long-term and more homogeneous neuronal differentiation in motor neuron–like NSC-34 cells. We found that the antimitotic drug cytosine arabinoside promoted robust and persistent neuronal differentiation in the entire cell population. Long and interconnecting neuronal processes with abundant growth cones were homogeneously induced and were durable for up to at least 6 weeks in culture. Moreover, cytosine arabinoside was permissive, dispensable, and mostly irreversible in priming NSC-34 cells for neurite initiation and regeneration after mechanical dislodgement. Finally, the expression of the cell proliferation antigen Ki67 was inhibited by cytosine arabinoside, whereas the expression levels of neuronal growth associated protein 43, vimentin, and motor neuron–specific p75, Islet2, homeobox 9 markers were upregulated, as confirmed by western blot and/or confocal immunofluorescence analysis. Overall, these findings support the use of NSC-34 cells as a motor neuron model for properly investigating neurodegenerative mechanisms and prospectively identifying neuroprotective strategies.

Key Words: cytosine arabinoside; Islet2; Hb9; Ki67; mitosis inhibition; neurite initiation; neurite regeneration; neuronal differentiation protocol; NSC-34; p75

Introduction

Culturing eukaryotic/prokaryotic cells under controlled experimental conditions has compelling applications in the study of cell growth and differentiation, virus infection, vaccine development, and the role of genes and pathways in health and disease (Allen et al., 2023). In a clinical context, cell culture is linked to creating model systems that dissect basic biology, replicate disease mechanisms, or define the efficacy or toxicity of novel drugs (Flobak et al., 2022). Among the advantages of using cell cultures for these applications, we note: their homogeneity and well-defined culture conditions greatly reducing the impact of genetic or environmental interfering variables; their consistency and reproducibility in data generation; and finally, their feasibility in manipulating genes, proteins, and pathways. The basic and translational applications of cultured cells are as diverse as those of cell types grown *in vitro*. Because the selection of a particular cell line and culture conditions depend on the emergent behavior and biological readout that we wish to investigate, the changes in cell size, shape, number, and selective transcription/translation events are among the key parameters that can be watchfully monitored in response to a mutable pathophysiological environment. The composition of the microenvironment is indeed critical for cell identity, morphogenesis, and function, by conditioning a specialized niche for the cells. However, we are still unaware of how selected environmental determinants can prime morphological shapes and functions.

[1]Experimental Neuroscience and Neurological Disease Models, IRCCS Fondazione Santa Lucia, Rome, Italy; [2]Institute for System Analysis and Computer Science "Antonio Ruberti" (IASI), National Research Council (CNR), Rome, Italy

†Current address: Università Cattolica del Sacro Cuore and IRCCS Fondazione Policlinico Universitario Agostino Gemelli, Largo A. Gemelli 8, 00168 Rome, Italy.

***Correspondence to:** Cinzia Volonté, PhD, cinzia.volonte@cnr.it.

https://orcid.org/0000-0001-7362-8307 (Cinzia Volonté)

Funding: *The present work was supported by FATALSDrug Project [Progetti di Ricerca@CNR SAC.AD002.173.058] from National Research Council, Italy (to CV).*

How to cite this article: *Vitale G, Amadio S, Liguori F, Volonté C (2025) Empowering the NSC-34 cell line as a motor neuron model: cytosine arabinoside's action. Neural Regen Res 20(0):000-000.*

Neurons allowing organisms to perceive their environment and act in response are the most morphologically varied phenotypes in the animal kingdom. Exposure to diverse types and concentrations of extracellular signals guides the selection of neuronal phenotypes, by regulating the expression of intrinsic determinants, particularly transcription factors, which in turn drive the fate of the neurons. Further knowledge of the molecular control of neuronal morphology and identity is therefore likely to be beneficial for understanding not only neural development, but also the causes/consequences of neurological defects and diseases. For instance, in the vertebrate spinal cord, motor neurons deregulate a common set of transcription factors at the progenitor stage (Olig2, Nkx6.1/6.2, and Pax6) and express a different set of transcription factors (homeobox 9 (Hb9), Islet1/2, and Lhx3) when they become postmitotic (Catela and Kratsios, 2021). Among the various models of motor neurons (Valetdinova et al., 2015), the hybrid NSC-34 cell line retains the ability to proliferate in culture while possessing properties expected for mature motor neurons, such as action potentials, neurofilament protein expression, acetylcholine synthesis, storage, and release (Cashman et al., 1992). By modeling features of motor neurons in an immortalized clonal system, these cells, however, do not elicit massive and homogeneous neuronal differentiation, moreover, sustained over a long period.

The aim of this work was thus to prime NSC-34 cells with a postmitotic phenotype that optimizes a consistent and stable neuritogenesis using ara-C, and to further legitimate their use as a motor neuron model in which to dissect neurodegenerative pathways and potentially identify neuroprotective strategies.

Methods

Ethics statement

The ethical approval was waived because this study did not include experiments in humans or in animal models and the cell line used is available commercially.

Cell culture

The NSC-34 cell clone (RRID: CVCL_D356) used in the present work (Cascella et al., 2022) was a kind gift from Department of Experimental and Clinical Biomedical Sciences "Mario Serio", University of Florence, Florence, Italy. NSC-34 cells were originally generated by fusion of aminopterin-sensitive mouse neuroblastoma N18TG2 cells with motor neuron–enriched embryonic day 12–14 mouse spinal cord cells (Cashman et al., 1992). NSC-34 cells were maintained in growth medium (GM) consisting of Dulbecco's modified Eagle's medium (DMEM)/F12 (Euroclone, Pero (MI), Italy, Cat# ECM0095) supplemented with 10% heat-inactivated fetal bovine serum (Euroclone, Cat# ECS0187L) and 1% penicillin/streptomycin, in a humidified 5% CO_2 atmosphere at 37°C. The culture medium was renewed twice a week and the cells were routinely passaged when they reached ~80% confluency, for a maximum of 40 passages. Experiments were routinely repeated and confirmed with both low (< 20) and high (> 20) passages.

Cell counting

The culture medium was removed from the cell plate and replaced with a 1 mL/35 mm dish of a detergent-containing lysing solution (0.05% ethyl-hexadecyl-dimethyl ammonium bromide, 0.028% acetic acid, 0.05% Triton X-100, 0.3 mM NaCl, 0.2 mM $MgCl_2$, in PBS, pH 7.4). After ~2 minutes at room temperature, the solution consisted of a uniform suspension of single, intact, viable nuclei. The solution was then collected, and the nuclei were counted with a hemocytometer. Broken or damaged nuclei were not included in the counts (Volonté et al., 1994).

Neuronal differentiation

For differentiation experiments, NSC-34 cells were plated at the density described in each figure legend, and in differentiation medium (DM) consisting of DMEM/F12 supplemented with 0.5% fetal bovine serum, 1% penicillin/streptomycin, and 1% modified Eagle's medium non-essential amino acids solution (Sigma-Aldrich, Darmstadt, Germany, Cat# M7145), in the presence of either 1 µM retinoic acid (RA; Cat# R2625), 100 µM dibutyryl-cyclic AMP (dBcAMP, Cat#D0260), 10 µM forskolin (Cat# F6886), 0.1–1 µM cytosine arabinoside (ara-C; Cat# C6645), 5 µg/mL and 1 ng/mL Cycloheximide (Cat# C7698) (all from Sigma-Aldrich) or 1 µg/mL-10ng/mL Actinomycin D (Cat# A7592) (Thermo Fisher Scientific, Waltham, MA, USA). All cell conditions were monitored at different time points and pictures were taken with Olympus IX50 inverted phase contrast microscope (Olympus, Tokyo, Japan) equipped with a digital image acquisition system (Bio Cell, Rome, Italy).

Neuronal quantification

After confocal immunofluorescence microscopy was performed with light neurofilament (NFL), beta3-tubulin, SMI32, and/or vimentin antibodies (**Table 1**), the images were processed with ImageJ software (1.54f version, https://imagej.net/software/imagej) and neuronal quantification was performed by the ImageJ plug-in Analyze Skeleton (3.4.2 version, https://imagej.net/plugins/analyze-skeleton). After the manufacturer's protocol application, the Analyze Skeleton plugin provides a tagged skeleton image from which the number of branches (segments), the junction points among branches, the length of the longest branch (µm), and the total extension of the neuronal network (µm) can be extrapolated from the resulting output files.

Neurite regeneration assay

After neuronal differentiation for 10–15 days in DM, in the presence of 0.5 µM ara-C, NSC-34 cells were rinsed three times with DMEM/F12 and then mechanically dislodged from the dish, by forceful trituration with a cell scraper. The cells were subsequently collected and gently drawn in and out, with a Pasteur pipette. As a result of this procedure, the neurites of the cells were completely lost by mechanical shearing and resorption into the cell body (D'Ambrosi et al., 2000). The cells were then replated in DM, in the presence or absence of ara-C, or in GM for an additional 10–20 days. They were observed and photographed at different time points. This procedure can be successfully repeated for a second cycle of neurite regeneration.

Table 1 | **Details and work dilutions of primary antibodies used for immunofluorescence (IF) and western blot (WB) analysis**

Host, antibody	IF dilution	WB dilution	Supplier	Cat#
Mouse, beta3-tubulin	1:500	–	Immunological Sciences, Rome, Italy	MAB-10288
Rabbit, ChAT	1:100	–	Merck Millipore, Temecula, CA, USA	AB143
Mouse, GAP43	1:1000	1:1000	MyBioSource, San Diego, CA, USA	MBS555937
Mouse, GAPDH	–	1:5000	Merck Millipore	CB1001
Mouse, Hb9	–	1:50	Santa Cruz Biotechnology, Dallas, TX, USA	SC515769
Mouse, Islet2	1:100	1:100	Santa Cruz Biotechnology	SC390746
Rabbit, Ki67	1:250	–	Thermo Fisher Scientific	MA514520
Mouse, MAP2	1:1000	–	Sigma-Aldrich, Darmstadt, Germany	M4403
Goat, NFL	1:100	–	Santa Cruz Biotechnology	SC12980
Rabbit, p75	1:50	1:1000	Abcam, Waltham, MA, USA	AB52987
Mouse, SMI32	1:1000	–	BioLegend, San Diego, CA, USA	801701
Rabbit, Vimentin	1:200	1:1000	Abcam	AB92547

ChAT: Choline acetyltransferase; GAP43: growth-associated protein 43; GAPDH: glyceraldehyde 3-phosphate dehydrogenase; Hb9: homeobox 9; MAP2: microtubule-associated protein 2; NFL: light neurofilament.

Total RNA extraction, reverse transcription, and quantitative PCR

NSC-34 cells were lysed with QIAzol (Qiagen, Hilden, Germany) according to the manufacturer's instructions. After genomic DNA elimination, reverse transcription was achieved using PrimeScript RT Reagent Kit with gDNA Eraser (Takara Bio, Shiga, Japan, Cat# RR047A). Quantitative PCR (qPCR) was carried out with TB Green® Premix Ex Taq™ (Takara Bio, Cat# RR420W) and relative quantification of the transcripts was determined by the $2^{-\Delta\Delta Ct}$ method (Livak and Schmittgen, 2001) with the TATA box binding protein used as reference gene. The thermal profile of qPCR reactions was declined as follows: initial denaturation at 95°C for 10 minutes, which was followed by 35 cycles of 10 seconds at 95°C and 30 seconds at 60°C. Melting curves were obtained after 10 seconds at 95°C and 1 minute at 65°C. At least three independent biological replicates were performed with three technical replicates each. The primers used were purchased from Sial (Rome, Italy). The sequences of primers used were as follows: (5′–3′): *Ki67*, forward: GAG GAG AAA CGC CAA CCA AGA G; reverse: TTT GTC CTC GGT GGC GTT ATC C. *TATA* box binding protein primers sequence (5′–3′): forward: CCA ATG ACT CCT ATG ACC CCT A; reverse: CAG CCA AGA TTC ACG GTA GAT.

Protein extraction and determination

Protein extraction and quantification were performed as described previously (Martire et al., 2020). Briefly, NSC-34 cells were harvested in RIPA buffer (1% Nonidet P40, 0.5% sodium deoxycholate, 0.1% SDS in PBS) and the protein concentration was determined by the Bradford method using Bio-Rad Protein Assay (Bio-Rad Laboratories, Segrate, Italy), and with bovine serum albumin as a standard. Cell lysates were added with the Laemmli sample buffer and boiled for 5 minutes.

Western blotting

Equal amounts of protein (15 µg) were loaded onto 10% polyacrylamide gels, separated by SDS-PAGE, and transferred to nitrocellulose membranes (Amersham Biosciences, Chicago, IL, USA) in a 20% ethanol-Tris-Glycine buffer. After 1-hour saturation with blocking solution consisting of 5% non-fat dry milk in TBS-T (10 mM Tris pH 8, 150 mM NaCl, 0.1% Tween 20), the membranes were incubated overnight at 4°C with the specified primary antibodies (**Table 1**) diluted in TBS-T buffer, and then for 1 hour at room temperature with HRP-conjugated secondary antibodies. HRP-linked anti-rabbit (Thermo Fisher Scientific, Waltham, MA, USA, Cat# 31460, RRID: AB_228341) and anti-mouse (Thermo Fisher Scientific, Cat# 31430, RRID: AB_228307) antibodies were diluted 1:5000. Bands were visualized using enhanced chemiluminescence ECL Advance Western blot detection kit (Amersham Biosciences) and iBright™ CL1000 (Thermo Fisher Scientific). Quantification of signal intensity was performed by ImageJ software.

Confocal immunofluorescence analysis and quantification

NSC-34 cells were fixed for 10 minutes in 4% paraformaldehyde, permeabilized in PBS containing 0.1% Triton X-100 and then incubated for 1.5 hours at 37°C with the specified primary antibodies (**Table 1**). The secondary antibodies (all purchased from Jackson ImmunoResearch, West Grove, PA, USA) diluted in PBS (1% normal donkey serum) were as follows: Cy3-conjugated donkey anti-rabbit IgG (1:100, Cat# 711-165-152, RRID: AB_2307443), Cy5-conjugated donkey anti-goat IgG (1:100, Cat# 705-175-147, RRID: AB_2340415), Alexa Fluor 488-AffiniPure donkey anti-mouse IgG (1:200, Cat# 715-545-151, RRID: AB_2341099), Alexa Fluor 488-AffiniPure donkey anti-rabbit IgG (1:200, Cat# 711-545-152, AB_2313584), and Alexa Fluor 555-AffiniPure donkey anti-mouse IgG (1:200, Cat# A32773). Höechst 33342 (Thermo Fisher Scientific, Cat# H1399) was used for nuclear staining (1:1000 in PBS). Images were acquired by a laser scanning confocal microscope (Zeiss, Jena, Germany, LSM800) equipped with four laser lines: 405 nm, 488 nm, 561 nm and 639 nm, as described previously (Amadio et al., 2017). The brightness and contrast of the digital images were adjusted using the Zen software (Zeiss) and quantified with ImageJ software (Apolloni et al., 2019).

Statistical analysis

Statistical analyses were performed using GraphPad Prism version 9.4.1 software (GraphPad Software, San Diego, CA, USA, www.graphpad.com). Statistical analysis of cell counting was performed by two-way analysis of variance and Dunnett's test for multiple comparisons. Western blot and qRT-PCR statistical analysis was performed by unpaired *t*-test. Statistical analysis of immunofluorescence acquisition was performed by one-way analysis of variance with Tukey's *post hoc* test for multiple comparisons. The data are expressed as mean ± SEM in **Figures 2A**, **6C**, **7A–D**, **Additional Figures 2A** and **3A**, while in **Figures 4A–D** and **6B** data are graphed with BoxPlot.

All statistical tests with corresponding significance levels are further specified in each figure legend indicating the specific *P* value of each test.

Results

The NSC-34 cells are a widely adopted motor neuron model, whose differentiation protocols have been extensively exploited. These mainly include low concentrations of serum (0.5%–1%) supplemented with either retinoic acid (RA, 1–10 μM (Stanzione et al., 2021; Ackerman and Gerhard, 2023; Wu et al., 2024)), or cAMP agents (10–100 μM (Nango et al., 2017)), prostaglandin (10–100 μM (Nango et al., 2020; Nango and Kosuge, 2022)), or deoxycholic acid (20 μM (Ackerman and Gerhard, 2023)). Under these conditions, only part of the cells differentiated into neurons with several spikes and various lengths neurites, while the majority continued dividing in culture and maintained a pleomorphic roundish, flat, or irregularly shaped morphology, however not exhibiting extensive and long-term neurite outgrowth.

The aim of our work was to promote a postmitotic phenotype displaying more homogeneous and long-term neuronal differentiation in NSC-34 cells.

We showed that NSC-34 cells grown in GM were heterogeneous in shape and exhibited variable proportions of spherical or irregularly flat cells bearing short spikes (**Figure 1A** and **B**). When cultured in DM, only very few cells elongated cellular processes that reached up to 5–8 cell bodies in length, by approximately day 3 (**Figure 1C**). After 7 days, these protrusions however withdrew, and the cells started duplicating again in culture (**Figure 1D**). By confirming previous results (Maier et al., 2013), we showed that RA (1 μM) potentiated not only the length of these processes, but also the percentage of neurite-bearing cells, which reached up to nearly 50% of the entire population, on day 3 (**Figure 1E**). However, on day 7 we confirmed that RA became highly toxic, causing cytoplasmic vacuolation, massive cell death, and debris, together with beading, retraction and clear deterioration of the neuritic branches (**Figure 1F**).

Stimulation of the cAMP pathway has previously been proven effective in boosting the neuronal differentiation of various cell lines, including NSC-34 (Aglah et al., 2008; Nango et al., 2017). We cultured these cells in DM and the simultaneous presence of dBcAMP, a cell-permeable cAMP analogue that inhibits cAMP phosphodiesterase and preferentially activates protein kinase A (Aglah et al., 2008). At the concentration of 100 μM, dBcAMP on day 3 caused the outgrowth of several visible processes (**Figure 1G**) that persisted for up to 7 days in culture (**Figure 1H**). However, at ~10 days, the neurites massively withdrew, and the cells started to duplicate in culture, as demonstrated by direct counting (data not shown) and by the presence of several clusters of newly generated roundish cells (**Figure 1I**). Corroborating these results, we now demonstrated that the drug forskolin (10 μM) stimulating the adenylate cyclase and acting via protein kinase A (Aglah et al., 2008), can induce a similar neuritogenic effect (**Figure 1J**). However, the neurites already acquired a beading appearance at 3 days (**Figure 1K**) and after 7 days some toxicity became evident (**Figure 1L**), while some surviving cells started duplicating again (**Figure 1M**).

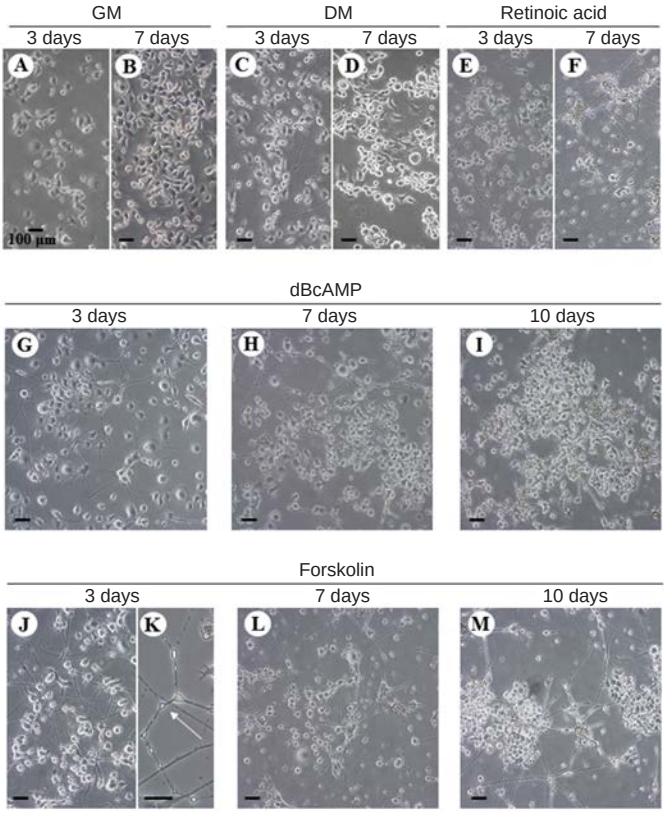

Figure 1 | **Only partial and transient neuritogenesis is induced by different agents in NSC-34 cells.**
NSC-34 cells were plated at 1×10^5 cells/35 mm dish and maintained in GM for 3 (A) and 7 (B) days, or in DM for 3 (C) and 7 (D) days. Moreover, they were maintained in DM supplemented with either 1 μM retinoic acid (RA) for 3 (E) and 7 (F) days, or 100 μM dBcAMP for 3 (G), 7 (H), and 10 (I) days, or 10 μM forskolin for 3 (J, K), 7 (L), and 10 (M) days. In K, white arrow shows neurite beading caused by forskolin. All the experimental conditions were repeated at least three times. Scale bars: 100 μm. dBcAMP: Dibutyryl-cyclic AMP; DM: differentiation medium; GM: growth medium.

The differentiating effect of cytosine arabinoside

To circumvent the long-term toxic effects of RA or the transient induction of neuronal differentiation by cAMP agents, we hypothesized that the inhibition of cell duplication *per se* could potentiate the frail neuronal differentiation from NSC-34 cells. The antimetabolite ara-C remains one of the most effective antiproliferative drugs used with duplicating cells. Its actions depend on the conversion to the triphosphate derivative ara-CTP, which is capable of interfering with DNA polymerases and is incorporated into elongating DNA strands, thus leading to DNA fragmentation, duplication chain termination, and eventually apoptosis when a threshold level of DNA damage is exceeded. The concentration of 0.1 μM ara-C for 2 days (**Figure 2A**) significantly inhibited NSC-34 cell duplication compared with the control DM condition. However, the number of cells in culture progressively increased thereafter, indicating that 0.1 μM ara-C sustains only a transient inhibition of cell proliferation. When ara-C was instead used at 0.25 or 0.5 μM, the antimitotic effect appeared to be highly stable (**Figure 2A**). Despite a large amount of cell death in DM alone at 24–96 hours after plating (Matusica et al., 2008), the cells roughly duplicated (~2×10^5) in DM alone after 2 days in culture, while in the presence of ara-C they were reduced by at least half (less

than 5 × 10^4) with respect to the time = 0, thus suggesting that ara-C does not attenuate cell death. However, ara-C at the dose of 0.5 µM prompted a sturdy neuritic arborization that gradually improved with time in culture. In particular, after 4 days the cells elongated more abundant and robust neurites (**Figure 2C**) compared with control 0 day (**Figure 2B**), and the neurites became a branching network after 7 days (**Figure 2D**). When ara-C was used at a concentration of 1 µM instead, it showed some levels of toxicity starting after 7–10 days and thereafter (data not shown).

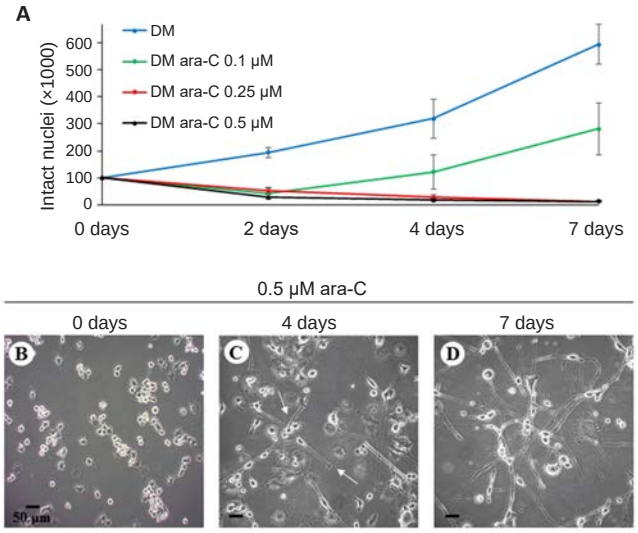

Figure 2 | Ara-C sustains a concentration-dependent and long-lasting neuronal phenotype in NSC-34 cells.
(A) NSC-34 cells were plated at 1 × 10^5 cells/35 mm dish in DM supplemented with different concentrations of ara-C for 2, 4, and 7 days. Data are expressed as mean ± SEM, *n* = 3 independent experiments. Statistical analysis was performed by two-way analysis of variance with Dunnett's *post hoc* test for multiple comparisons. All time points referred to T0 (0 days) for DM and for each ara-C concentration. They are statistically significant, with the exception of 0.1 µM ara-C at T4 (4 days) and T7 (7 days). T2 (2 days) DM ***P* = 0.0013; T4 DM ***P* = 0.0096; T7 DM ***P* = 0.0084; T2 DM-ara-C 0.1 µM ****P* = 0.0001; T2 DM ara-C 0.25 µM **P* = 0.0233; T4 DM-ara-C 0.25 µM **P* = 0.0123; T7 DM-ara-C 0.25 µM ****P* = 0.0004; T2 DM-ara-C 0.5 µM **P* = 0.0105; T4 DM-ara-C 0.5 µM ****P* = 0.0007; T7 DM-ara-C 0.5 µM ****P* = 0.0010. (B–D) NSC-34 cells were plated at 2 × 10^5 cells/60 mm dish in DM supplemented with 0.5 µM ara-C for 0, 4, and 7 days. In C, white arrows indicate growth cones. Scale bars: 50 µm. ara-C: Cytosine arabinoside; DM: differentiation medium.

Dissecting cytosine arabinoside-dependent neuritogenesis

To investigate the mechanisms related to the ara-C-induced differentiation of NSC-34 cells, we adopted a pharmacological approach and tested some DNA/RNA intercalating agents. Actinomycin D inhibiting DNA-primed RNA synthesis by blocking rRNA and heterogeneous nuclear RNA production, and cycloheximide blocking tRNA binding and release from ribosomes, both interfered with neuritogenesis when used at 10–1000 ng/mL and 1–5000 ng/mL respectively, thus suggesting that novel transcription and protein synthesis are indeed required for maintaining healthy neurites. In particular, at the highest tested concentration of 1 µg/mL, actinomycin D *per se* induced massive death within 24 hours (**Additional Figure 1A**) and total cell loss after 2 further days (data not shown). At the lowest and suboptimal concentration tested of 10 ng/mL, the spikes and short neurites that were visible after 2 days of actinomycin D treatment (**Additional Figure 1B**) remained quite stable for 2 additional days (**Additional Figure 1C**), while they retracted in 3 more days, accompanied by total cell death (data not shown). In the presence of cycloheximide at the highest tested concentration of 5 µg/mL, some cells elongated short- and medium-length spikes whitin 24 hours (**Additional Figure 1D**), but the cells remained viable only for 2–3 further days (data not shown). When tested at suboptimal 1 ng/mL concentration, cycloheximide induced a mild neuritogenic effect after 2 days of treatment (**Additional Figure 1E**), but a clear increase of cell density was visible after about 2 further days (**Additional Figure 1F**). Finally, we investigated drugs interfering with microtubule stability. As expected, colchicine preventing microtubule assembly (used at 1 ng/mL), taxol stabilizing microtubules and reducing their dynamicity (used at 10-1000 nM), and vinblastine destabilizing microtubules at minus ends while stabilizing microtubules at plus ends (used at 1 nM), all prevented or inhibited neuritogenesis after 2–3 days (data not shown).

Next, we characterized the biological response of NSC-34 cells to ara-C by performing confocal immunofluorescence analysis of NFL (**Figure 3A–C**), beta3-tubulin (**Figure 3D–F**), and nonphosphorylated high neurofilament (SMI32) proteins (**Figure 3G–I**, **H1–H3**). Approximately 2 hours after plating and cell adhesion to the substrate (T0), the NFL and SMI32 antibodies stained mainly the cytoplasm and the very short spikes protruded from NSC-34 cells cultured with 0.5 µM ara-C (**Figure 3A** and **G**). On day 4 (T4), ara-C prompted a typical neuronal pattern that differed in size, shape, immunofluorescence intensity, and number/length of arborizations per cell (**Figure 3B** and **3H**). In detail, the NFL signal was increased in the enlarged cell bodies and in the protrusions already emerging at this stage (**Figure 3B**). Moreover, at higher magnification (**Figure 3H1–H3**), the SMI32 immunopositive staining highlighted different subcellular structures: the red arrows indicate neurites and growth cones present at the edge of the neuritic processes (**Figure 3H1**); the white arrow highlights radial structures within the cytoplasm, in addition to neurofilament accumulations which are possibly indicative of budding protrusion structures (**Figure 3H2**); the yellow arrow delineates the nuclear membrane (**Figure 3H3**). At 14 days (T14, **Figure 3I**), the majority of the cells possessed long SMI32 bipolar or radial immunopositive neurites. By correlating with the phases of neurogenesis, the marker of neuronal identity beta3-tubulin was highly increased in NSC-34 cells maintained in culture in the presence of 0.5 µM ara-C for 4 days (**Figure 3E**) compared with T0 (**Figure 3D**) and it underlined the thick neuritic branches and growth cones at T14 (**Figure 3F**).

Quantification of cytosine arabinoside-dependent neuritogenesis

To provide quantitative evidence of the neuritogenic effect induced by ara-C, the immunofluorescence images acquired with NFL, beta3-tubulin, and SMI32 antibodies were next quantified with ImageJ Analyze Skeleton plugin. We measured:

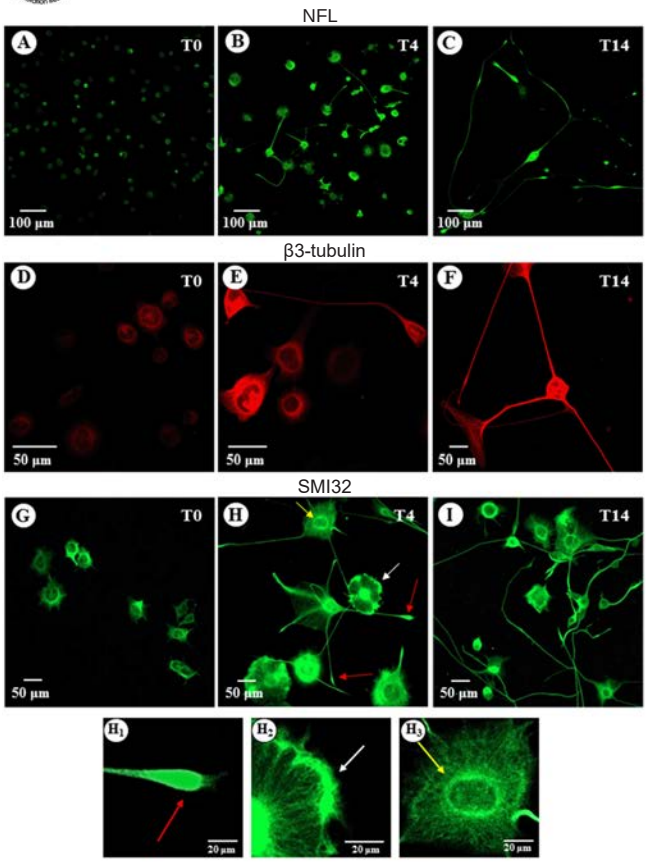

Figure 3 | **Neuronal characterization of ara-C-treated NSC-34 cells.**
NSC-34 cells were plated at 1 × 10^5 cells/35 mm dish in growth medium and analysis was performed at 2 hours after plating (T0; A, D, G), or maintained in differentiation medium supplemented with 0.5 µM ara-C for 4 (T4; B, E, H) and 14 (T14; C, F, I) days. Representative images after immunofluorescence confocal microscopy are shown. Panels H1-H3 represent higher magnification details of views of H at the points of the colored arrows. The red arrows highlight growth cones, the white arrow shows radial structures within the cytoplasm, and the yellow arrow indicates the nuclear membrane. Scale bars: 100 µm in A–C, 50 µm in D–I, and 20 µm in H1–H3. ara-C: Cytosine arabinoside; NFL: light neurofilament.

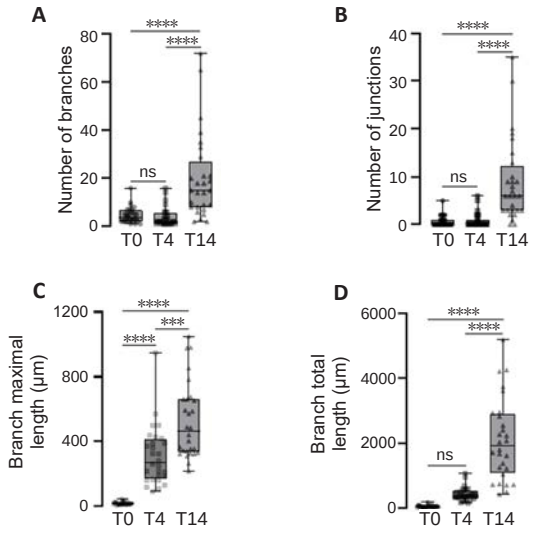

Figure 4 | **Neuronal quantification of ara-C-treated NSC-34 cells.**
NSC-34 cells were plated at 1 × 10^5 cells/35 mm dish in growth medium and analysis performed at 2 hours after plating (T0) or maintained in differentiation medium supplemented with 0.5 µM ara-C for 4 and 14 days (T4 and T14, respectively). Quantification of the number of neuritic branches (A), junction points (B), average maximal length (µm) of branches (C), and average total extension (µm) of the neuritic network (D) was performed with ImageJ Analyze Skeleton ImageJ plug-in on confocal immunofluorescence images. Data are shown as box and whisker plots of n = 5 independent experiments, with 28 total cells analyzed at each time point. Statistical analysis was performed by two-way analysis of variance with Tukey's *post hoc* test for multiple comparisons. In A, T4/T0 not significant (ns); T14/T0 ****P = 0.000005; T14/T4 ****P = 0.000002. In B, T4/T0 ns; T14/T0 ****P = 0.0000005; T14/T4 ****P = 0.0000006. In C, T4/T0 ****P = 0.0000008; T14/T0 ****P = 0.0000000000006; T14/T4 ***P = 0.0002. In D, T4/T0 ns; T14/T0 ****P = 0.0000000000006; T14/T4 ****P = 0.0000000001. ara-C: Cytosine arabinoside.

the number of neuritic branches (segments) elongating from both the cell soma and each junction point (**Figure 4A**); the number of junction points among segments (**Figure 4B**); the average of the maximal length (µm) of each segment in each cell (**Figure 4C**); finally, the average of the total length (µm) of all segments in each cell, e.g., the total extension of the neuritic network for each cell (**Figure 4D**). While the spike/neurite-possessing cells increased from ~18% at T0 to ~36% at T4, and to ~80% at T14 in the presence of ara-C, the numbers of branches and junctions remained nearly similar between T0 and T4, while they both markedly increased at T14. Moreover, the maximal and total length of branches progressively increased with time in culture in the presence of ara-C, reaching respectively 300 µm and 400 µm in length at T4, and 520 µm and 2 mm in length at T14. This represents a relevant improvement with respect to the treatment with DM alone or RA, which induced an average neurite length in differentiated neurons of ~200 µm at T6 (Carletti et al., 2011), and ~105 µm at T4 (Maier et al., 2013), respectively.

Long-lasting neuritogenesis promoted by cytosine arabinoside

Long-lasting neuronal differentiation is mandatory for legitimating the use of NSC-34 cells as a motor neuron model to dissect neuritogenesis, neurodegenerative mechanisms, and neuroprotective strategies. Thus, we cultured NSC-34 cells in DM supplemented with ara-C for longer time intervals. Notably, the bushy network of highly interconnecting neurite branches that were already evident after ara-C treatment for 7 and 14 days (**Figures 2D** and **3C**, **3F**, **3I**, respectively) remained consolidated and fully preserved for up to at least 6 weeks in culture (**Figure 5A–D**). While very long neurites persisted in the majority of the cell population for up to 8 weeks in culture (data not shown), at the latest times shown (6 weeks, **Figure 5D**) some neurites started appearing thinner and in part fragmented (**Figure 5D**), some cell bodies initiated shrinking, and cell debris and slight death could also be observed as a sign of aging in culture. We next investigated whether the neuronal commitment induced by ara-C could be sustained even after the removal of ara-C. We demonstrated that after 10 days in the continuous presence of 0.5 µM ara-C (but not 0.1 µM, data not shown), NSC-34 cells could be switched to DM without ara-C and they did not duplicate in culture for at least 15 additional days, as directly quantified by counting intact viable nuclei (**Additional Figure 2A**) and, importantly,

they still preserved the neuron-like phenotype (**Figure 5B**), for up to at least 30 days in culture (data not shown). In other words, they became "neuronal primed" by eliciting a stable neuronal phenotype. Moreover, if switched to GM (without ara-C) some cells visibly escaped from the mitotic arrest and triplicated in about 15 further days (**Additional Figure 2A**), while others still preserved a neuronal phenotype (**Additional Figure 2B**). This finding suggests that once differentiated, the cells maintain a post mitotic trait and/or a silent staminality only in the absence of serum factors. The neuritogenic action of 0.5 µM ara-C was remarkably maintained also in DM completely without serum for at least 15 days (data not shown).

The neurite regeneration paradigm

Having established that NSC-34 cells become "neuronal primed" by ara-C, we next investigated the paradigm of neurite regeneration, a reparative process not requiring new RNA synthesis. In detail (**Figure 5I**), ara-C fully differentiated cells (0.5 µM for 10 days) were detached from the culture plate and the neurites dismantled. When replated even in the absence of ara-C, the cells adhered to the substrate in 2 hours, and appeared healthy and in good condition (data not shown). On day 1 (**Figure 5E**), the cells regrew novel processes of variable length and thickness, ending with several visible growth cones (arrows). On day 3 (**Figure 5F**), the cells underwent full neurite regeneration that persisted for at least 20 days (**Figure 5G**) in the absence of ara-C. Moreover, regenerated neuronal processes were morphologically indistinguishable from ex novo neurites grown in culture for 3–4 weeks (compare **Figure 5G** with **Figure 5B** and **C**). Remarkably, the neurite regeneration process could be repeated and sustained at least twice in a row (**Figure 5H**) and the neurites persisted for at least 8 further days in the complete absence of ara-C (inset in **Figure 5H**). These findings demonstrate that ara-C-primed NSC-34 cells mechanically deprived of neurites remain capable of autonomously reshaping and maintaining their full neuritic network.

Neuronal specification markers

To better characterize ara-C-differentiated NSC-34 cells, we performed qPCR, western blot, and confocal immunofluorescence analysis, using primers and antibodies that recognize markers of either duplication, pan-neuronal, or motor neuronal commitment. We demonstrated that the validated nuclear marker of proliferating tumor cells responsible for heterochromatin organization (Scholzen and Gerdes, 2000; Sobecki et al., 2016), Ki67, significantly and progressively decreased at T4 and T14 after treatment with 0.5 µM ara-C, as shown by immunofluorescence and qPCR analysis (**Figure 6**). Moreover, the intensities of the neuronal proteins growth associated protein 43 (GAP43) and vimentin increased, as demonstrated by both western blot and confocal analysis (**Figure 7A** and **B**). More specific early motor neuron markers such as p75 and Islet2 were also significantly modulated by treatment with ara-C (**Figure 7C** and **D**). In detail, the low-affinity p75-NGF receptor is a protein exclusively expressed by motor neurons in the spinal cord, also used to isolate embryonic motor neurons from the lumbar spinal cord (Wiese

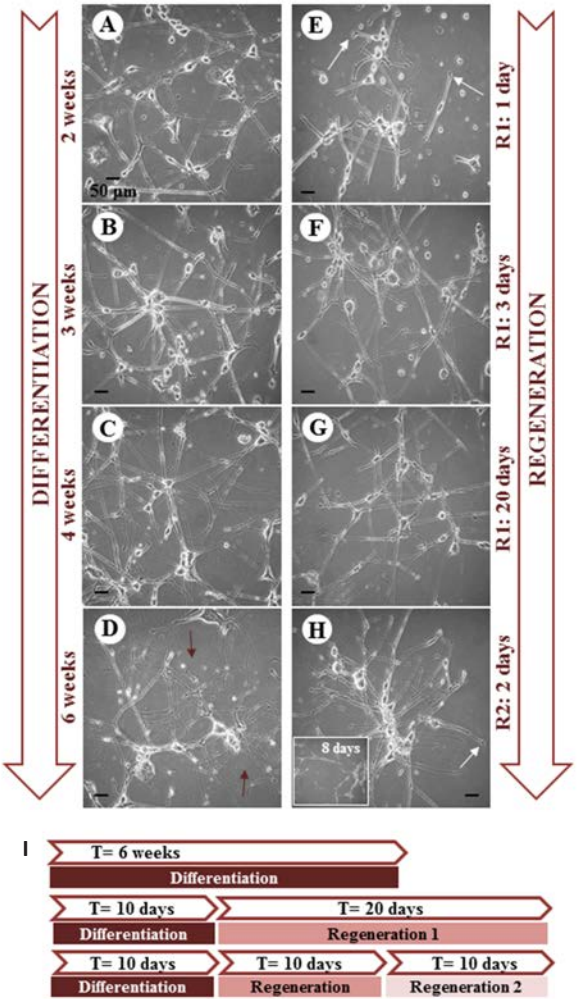

Figure 5 | Long-lasting neurite initiation and regeneration are induced by ara-C.

NSC-34 cells were plated at 1×10^6 cells/90 mm dish and maintained for 2 (A), 3 (B), 4 (C), or 6 (D) weeks in differentiation medium supplemented with 0.5 µM ara-C. (E–G) After 10 days of differentiation in the presence of 0.5 µM ara-C, the cells were harvested, replated in a 60 mm dish, and observed after 1 (E), 3 (F) and 20 (G) days (R1, first round of regeneration). (H) After neurite regeneration for 10 days, the cells were exposed to a second round of neurite regeneration (R2) and observed at 2 (H) and 8 (inset in H) days. In panel D red arrows show thin and fragmented neurites; in panels E and H white arrows indicate growth cones. (I) The schematic representation of differentiation and regeneration is shown. Scale bars: 50 µm. The differentiation images are representative of at least $n = 4$ independent experiments and the regeneration images of $n = 3$ independent experiments are shown. ara-C: Cytosine arabinoside.

et al., 2010). NSC-34 cells fully differentiated by ara-C for 14 days displayed increased immunoreactivity for p75 protein (**Figure 7C**). The transcription factor involved in neuronal fate Islet2 (Tsuchida et al., 1994) was instead significantly but transiently upregulated after 4 days in the presence of ara-C (**Figure 7D**). The transcription factor Hb9, described as a spinal cord motor neuron-specific marker and critical protein for postmitotic specification, was also transiently induced by ara-C after western blot analysis (**Additional Figure 3A**). Finally, the immunofluorescence intensity of the choline acetyltransferase enzyme (ChAT), which is responsible for acetylcholine biosynthesis in motor neurons, was highly

increased by ara-C after 4 days of treatment, while both cell bodies and abundant neuritic branches were strongly delineated after 14 days (**Additional Figure 3B** and **D**). The same occured for the neuron-specific cytoskeletal protein MAP2 enriched in dendrites and perikarya (**Additional Figure 3C** and **D**).

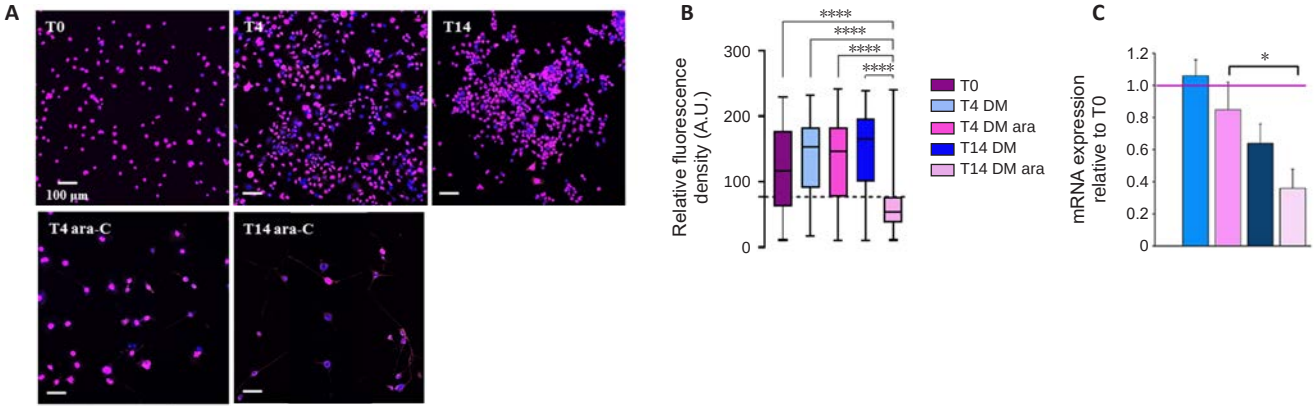

Figure 6 | **Ki67 proliferation marker is down regulated by treatment with ara-C.**
(A) NSC-34 cells were plated at 1 × 10^5 cells/35 mm dish in growth medium, and analysis performed at 2 hours after plating (T0) or maintained in differentiation medium (DM) supplemented without or with 0.5 µM ara-C for 4 and 14 days (T4 DM and T14 DM, respectively). Representative images of immunofluorescence confocal microscopy performed with Ki67 antibody are shown (scale bar: 100 µm). (B) Quantification of fluorescence intensity was performed with ImageJ software and represented as a box and whisker plot of relative density (A.U., arbitrary units) (n = 3). Statistical analysis was performed by two-way analysis of variance with Tukey's *post hoc* test for multiple comparisons: T14 DM ara-C/T0 ****P = 0.0000000004; T14 DM ara-C/T4 DM ****P = 0.0000000004; T14 DM ara-C/T4 DM ara-C ****P = 0.0000000004; T14 DM ara-C/T14 DM *****P = 0.0000000004. The dotted line indicates the 75th percentile of the T14 DM ara-C sample. (C) qRT-PCR analysis of Ki67 transcript in ara-C treated and untreated NSC-34 cells at T4 and T14. Transcript levels were normalized to TATA box binding protein gene and are represented as fold change relative to T0 cells (indicated by the purple horizontal line and set to 1). Bar graphs (T4 DM = light blue; T4 DM ara = pink; T14 DM = blue; T14 DM ara = light pink) represent mean ± SEM of at least three independent replicates. Statistical significance was calculated by unpaired t-test (*P = 0.0375). ara-C: Cytosine arabinoside.

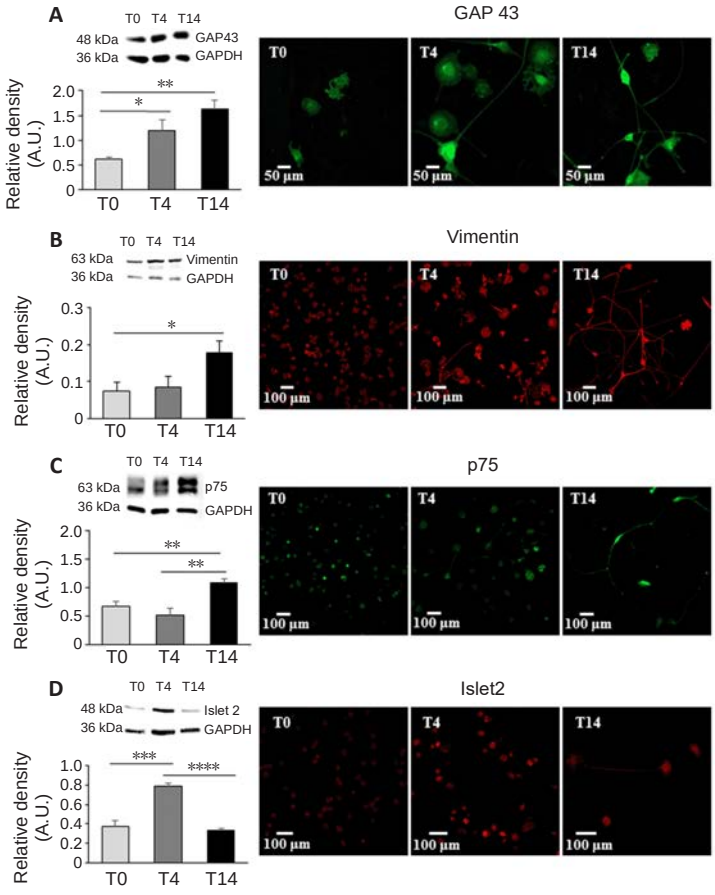

Figure 7 | **Neuronal and motor neuronal markers are induced by ara-C.**
For western blot analysis, NSC-34 cells were plated in growth medium (GM) at 1.5 × 10^5 cells/90 mm dish and protein extracted at 2 hours after plating (T0) or plated at 5 × 10^5 cells/90 mm dish and maintained in differentiation medium supplemented with 0.5 µM ara-C for 4 days (T4), or plated at 1 × 10^6 cells/90 mm dish and maintained in differentiation medium supplemented with 0.5 µM ara-C for 14 days (T14). Proteins were extracted and subjected to SDS-PAGE and western blot. GAP43 (A) and Islet2 (D) analyses represent mean ± SEM of n = 4 experiments, while Vimentin (B) and p75 (C). Bar graphs represent the mean ± SEM of n = 3 experiments. Relative density (A.U., arbitrary units) was expressed as the ratio between the intensity of each target and GAPDH intensity, used as loading control. Statistical analysis was performed by the unpaired t-test. In A, GAP43: T4/T0 *P = 0.03; T14/T0 **P = 0.002; T14/T4 not significant. In B, Vimentin: T4/T0 not significant; T14/T0 *P = 0.05; T14/T4 not significant. In C, p75: T4/T0 not significant ; T14/T0 **P = 0.006; T14/T4 **P = 0.006. In D, Islet2: T4/T0 ***P = 0.0007; T14/T0 not significant; T14/T4 ****P = 0.00002. For immunofluorescence analysis, NSC-34 cells were plated at 1 × 10^5 cells/35 mm dish in GM, and analysis performed at 2 hours after plating (T0) or maintained in DM supplemented with 0.5 µM ara-C for 4 (T4) and 14 (T14) days. Representative images of immunofluorescence confocal microscopy at different time points are shown. Green staining was used to visualize GAP43 (Panel A) and p75 (Panel C) markers, while red staining was used for Vimentin (Panel B) and Islet 2 (Panel D). Scale bars: 50 or 100 µm, as indicated. ara-C: Cytosine arabinoside; GAP43: growth associated protein 43; GAPDH: glyceraldehyde 3-phosphate dehydrogenase.

Discussion

Familial/sporadic neurodegenerative diseases targeting upper and/or lower motor neurons are divided into three major diagnostic categories of amyotrophic lateral sclerosis (Akçimen et al., 2023), primary lateral sclerosis (Marzoughi et al., 2023), and progressive muscular atrophy (Marchioretti et al., 2023). Moreover, they comprise progressive bulbar/pseudobulbar palsy, hereditary spastic paraplegia, Kennedy's disease, hereditary motor neuropathies, and post-polio syndrome, all sharing major impairment of the motor neuron-muscle unit, together with muscle atrophy and severe palsy, irremediably resulting in the death of patients (Foster and Salajegheh, 2019; Chaudhary et al., 2022). Regrettably, they also share a paucity of information about discriminative features and underlying mechanisms. The possibility of mimicking development, decline, and concomitant potential recovery in cell models, has become a primary step for discerning the different causes and modalities of motor neuron degeneration, and identifying more effective and disease-oriented therapeutic strategies (Adami and Bottai, 2019; Liguori et al., 2021). However, the low yields and inadequate purity of primary motor neuron preparations have impeded the elucidation of the unique biology and pathology of these neurons. The availability of an immortal and clonally homogeneous cell line, particularly the NSC-34 established by Cashman and coauthors (Cashman et al., 1992; Durham et al., 1993), has of course surmounted several of the technical obstacles related to the use of motor neurons in primary culture. Indeed, NSC-34 cells are a hybrid mouse motor neuron/neuroblastoma cell line retaining full ability to proliferate *in vitro* and, at the same time, expressing motor neuron features such as the presence of glutamate receptors, neurofilament triplet/vimentin proteins, a functional machinery for acetylcholine synthesis, storage and release, exactly as occurring during development (Cashman et al., 1992). However, because of their proliferation-differentiation dichotomy not exclusively generating differentiated neuronal cells, NSC-34 cells can present some limitations in mimicking motor neurons *in vitro*. Most importantly, their potentiality of homogeneous and long-term neuritogenesis has been very poorly investigated so far.

Gaining further insights into a durable and uniform process of neuronal differentiation accompanied by mitotic arrest might indeed become mandatory for studying and understanding motor neuron growth, degeneration, and regeneration, by the use of NSC-34 cells. This was the key aim of our work that has indeed established that the antimitotic drug ara-C, different from low serum concentrations (Matusica et al., 2008), retinoic acid (Ackerman and Gerhard, 2023), cAMP increasing agents (Nango et al., 2017), or prostaglandins (Nango et al., 2020), can effectively promote and sustain a robust and very time-persistent neuronal differentiation of these cells. A fundamental prerogative of ara-C in this context is the phenotypic "fidelity," meaning that morphological features induced by ara-C in NSC-34 cells, such as large-size soma with numerous long interconnecting neuronal processes and abundant growth cones, are induced homogeneously throughout the entire cell population and are, furthermore, permanent for up to at least 6 weeks in culture. Moreover, we have shown here that ara-C is: a) necessary and sufficient to empower neurite outgrowth; b) best effective in both inhibiting cell duplication and inducing neuritogenesis; c) permissive, but also dispensable, in priming NSC-34 cells for neuritogenesis; and d) mostly irreversible.

In light of these overall features, additional properties of ara-C deserve consideration. Ara-C is a potent antimitotic and chemotherapeutic agent used in the management and treatment of leukemias and lymphomas (Aldoss et al., 2008; Gökbuget and Hoelzer, 2009; Burnett et al., 2011), moreover known to induce the differentiation, for instance of human acute/chronic myelogenous leukemia cells into erythrocytes (Takagaki et al., 2005; Boudny and Trbusek, 2020) and of embryonic rhabdomyosarcoma cells into muscles (Crouch et al., 1993). However, this is the first evidence of ara-C inducing neuritogenesis, while its cytotoxicity definitely spares differentiating NSC-34 cells. Moreover, mitotic arrest and interference with cell duplication by ara-C are fully permissive for the motor neuron identity of NSC-34 cells, perhaps favoring their postmitotic status. We speculate that in the presence of ara-C the intrinsic motor neuron nature of NSC-34 cells prevails over the neuroblastoma tumorigenic feature. It is interesting to note that for instance cycloheximide at a concentration normally inhibiting translation induces per se the formation of only short-lived and short-length spikes, then becoming toxic in a few days. This finding suggests that NSC-34 cells do not require novel protein synthesis for initiating their innate neuritogenic program, but only for sustaining it over time, perhaps in compliance with the regular turnover of proteins necessary for neuritogenesis. Finally, the neuritogenic effect in NSC-34 cells depends on both mRNA transcription (not being sustained in the presence of actinomycin D), and microtubule dynamics, since compounds interfering with microtubule polymerization and stability such as colchicine, Taxol, and vinblastine, indeed prevent neuritogenesis.

Neuronal differentiation is known to be regulated by complex mechanisms mediated by intrinsic and extrinsic factors, comprising not only terminal mitosis as clearly sustained by ara-C, but also augmented expression of the phenotype-specific neurotransmitter machinery, cytoskeleton network, and synaptic structures. One further aim of our work was indeed to characterize how ara-C promotes and coordinates diverse groups of neuritogenic responses in NSC-34 target cells. In particular, we demonstrated that the potent effect of ara-C on neurite initiation and long-term maintenance comprises the modulation of pan-neuronal protein markers. Among these, we report for instance NFL, beta3-tubulin, SMI32, GAP43, vimentin, and MAP2. Some specific motor neuron markers are also regulated by ara-C, such as p75 receptor, modulating postmitotic neuronal survival decision, and required to organize the neuromuscular synapse by regulating synaptic vesicle availability (Pérez et al., 2019); Islet2, an early marker for motor neuron differentiation (Tsuchida et al., 1994); the homeodomain factor Hb9, an early postmitotic marker critical in consolidating motor neuron identity (Arber et al., 1999); and finally, the classical acetylcholine synthetic enzyme at the neuromuscular junction, ChAT, which is known to be absent in the tumoral-cell parent N18TG2 neuroblastoma line (Cashman et al., 1992). The

increased expression of these same markers is surely linked to the concomitant progressive downregulation of the cell proliferation marker Ki67 present during the active phases of the cell cycle and highly reduced in quiescent cells (Takagi et al., 2014), as we have indeed demonstrated.

A singularity acquired by ara-C-treated NSC-34 cells is "neuronal priming", i.e., the ability to promptly regrow sturdy neurites and regenerate a complex neuronal network when the cells are deprived of previously elongated neurites by mechanical derangement. Of note, this regenerating aptitude becomes a feature very relevant in light of the use of ara-C-primed NSC-34 cells as a motor neuron model for studying neurodegeneration and neurorepair, particularly for exploiting potential neuroprotective and/or regenerative strategies.

Although the chain of events regulating the neuronal differentiation of NSC-34 cells remains to be fully elucidated, the use of ara-C that we have demonstrated here offers the opportunity to bypass, for the first time, the dual and hybrid motor neuron/tumorigenic-neuroblastoma behavior of these cells, and to work with a homogeneous, fully differentiated, and over time-sustained neuronal phenotype. As such, treatment with ara-C stands as a methodological improvement for reliably dissecting morphological changes, neurite sprouting, survival, and cell death, and for pharmacologically manipulating neurodegeneration and regeneration within a simple, straightforward and, most importantly, well-grounded culture system reproducing motor neuron features. Previous studies have described for instance the motor neuron-differentiating versatility of human ESCs (Imamura et al., 2021) and iPSCs (Garone et al., 2022), the motor neuron direct-lineage reprogramming of fibroblasts (Qin et al., 2018), and the small molecule-based procedure for motor neuron reprogramming of astrocytes (Zhao et al., 2020), among the available approaches for overcoming the difficulty and inefficiency of working with primary motor neuron cultures. Although very viable, these methods based on genetic manipulation, repeated viral infection, and chemical manipulations are otherwise complicated, time-consuming, often inefficient, and in some cases hazardous, very expensive and ethically disputable when applicable. Compared with these methods, the use of ara-C for obtaining durably differentiated NSC-34 motor neurons is by far preferable for easiness, efficiency, and cost-effectiveness. Finally, yet importantly, mutual microglia-, astrocyte-, oligodendrocytes, or muscle-neuron cellular interactions can be more trustfully analyzed by the use of ara-C-differentiated NSC-34 cells in co-cultures (Ramya et al., 2023). While in our work we have highlighted a clear advancement in the exploitation of the NSC-34 cell line as a motor neuron model, the treatment with ara-C may, however, poses slight limitations in terms of yield, due to its structural nature as antimetabolite-causing cell death of rapidly dividing cells.

In conclusion, we have provided arguments and evidence that ara-C-primed NSC-34 cells constitute a very suitable preclinical model for studying motor neuron degenerative and regenerative events to identify novel mechanisms, markers, and therapeutics, i.e., the major motivation in motor neuron research. We believe that by validating and empowering the NSC-34 cell line through our new findings, we can now further explore the known unknowns of motor neuron degeneration and related diseases.

Acknowledgments: *This work was motivated in the memory of a great scientist, Prof. Justin J. Yerbury, whom we admire for courage, keen determination and pioneering studies on protein aggregation in motor neuron diseases, carried out also thanks to the NSC-34 cell model. We thank Prof. Fabrizio Chiti, Department of Experimental and Clinical Biomedical Sciences "Mario Serio", University of Florence, Florence, Italy for the kind gift of NSC-34 cells.*

Author contributions: *CV designed the study; GV, SA, and FL performed the study; GV, FL, and SA analyzed the data; CV wrote the paper. All authors read, contributed, and approved the final version of the manuscript.*

Conflicts of interest: *The authors declare no conflicts of interest.*

Data availability statement: *All relevant data are within the paper and its Additional files.*

Additional files:

Additional Figure 1: *In NSC-34 cells, actinomycin D and cycloheximide interfere with neuritogenesis.*

Additional Figure 2: *Cytosine arabinoside is dispensable after priming a stable neuronal phenotype in NSC-34 cells.*

Additional Figure 3: *Hb9, ChAT and MAP2 markers are modulated by cytosine arabinoside in NSC-34 cells.*

References

Ackerman HD, Gerhard GS (2023) Bile acids induce neurite outgrowth in Nsc-34 Cells via TGR5 and a distinct transcriptional profile. Pharmaceuticals (Basel) 16:174.

Adami R, Bottai D (2019) Spinal muscular atrophy modeling and treatment advances by induced pluripotent stem cells studies. Stem Cell Rev Rep 15:795-813.

Aglah C, Gordon T, Posse de Chaves EI (2008) cAMP promotes neurite outgrowth and extension through protein kinase A but independently of Erk activation in cultured rat motoneurons. Neuropharmacology 55:8-17.

Akçimen F, Lopez ER, Landers JE, Nath A, Chiò A, Chia R, Traynor BJ (2023) Amyotrophic lateral sclerosis: translating genetic discoveries into therapies. Nat Rev Genet 24:642-658.

Aldoss IT, Weisenburger DD, Fu K, Chan WC, Vose JM, Bierman PJ, Bociek RG, Armitage JO (2008) Adult Burkitt lymphoma: advances in diagnosis and treatment. Oncology (Williston Park) 22:1508-1517.

Allen SL, Elliott BT, Carson BP, Breen L (2023) Improving physiological relevance of cell culture: the possibilities, considerations, and future directions of the ex vivo coculture model. Am J Physiol Cell Physiol 324:C420-427.

Amadio S, Parisi C, Piras E, Fabbrizio P, Apolloni S, Montilli C, Luchetti S, Ruggieri S, Gasperini C, Laghi-Pasini F, Battistini L, Volonté C (2017) Modulation of P2X7 receptor during inflammation in multiple sclerosis. Front Immunol 8:1529.

Apolloni S, Caputi F, Pignataro A, Amadio S, Fabbrizio P, Ammassari-Teule M, Volonté C (2019) Histamine Is an Inducer of the Heat Shock Response in SOD1-G93A Models of ALS. Int J Mol Sci 20:3793.

Arber S, Han B, Mendelsohn M, Smith M, Jessell TM, Sockanathan S (1999) Requirement for the homeobox gene Hb9 in the consolidation of motor neuron identity. Neuron 23:659-674.

Boudny M, Trbusek M (2020) ATR-CHK1 pathway as a therapeutic target for

acute and chronic leukemias. Cancer Treat Rev 88:102026.

Burnett A, Wetzler M, Löwenberg B (2011) Therapeutic advances in acute myeloid leukemia. J Clin Oncol 29:487-494.

Carletti B, Passarelli C, Sparaco M, Tozzi G, Pastore A, Bertini E, Piemonte F (2011) Effect of protein glutathionylation on neuronal cytoskeleton: a potential link to neurodegeneration. Neuroscience 192:285-294.

Cascella R, Bigi A, Riffert DG, Gagliani MC, Ermini E, Moretti M, Cortese K, Cecchi C, Chiti F (2022) A quantitative biology approach correlates neuronal toxicity with the largest inclusions of TDP-43. Sci Adv 8:eabm6376.

Cashman NR, Durham HD, Blusztajn JK, Oda K, Tabira T, Shaw IT, Dahrouge S, Antel JP (1992) Neuroblastoma x spinal cord (NSC) hybrid cell lines resemble developing motor neurons. Dev Dyn 194:209-221.

Catela C, Kratsios P (2021) Transcriptional mechanisms of motor neuron development in vertebrates and invertebrates. Dev Biol 475:193-204.

Chaudhary R, Agarwal V, Rehman M, Kaushik AS, Mishra V (2022) Genetic architecture of motor neuron diseases. J Neurol Sci 434:120099.

Crouch GD, Kalebic T, Tsokos M, Helman LJ (1993) Ara-C treatment leads to differentiation and reverses the transformed phenotype in a human rhabdomyosarcoma cell line. Exp Cell Res 204:210-216.

D'Ambrosi N, Cavaliere F, Merlo D, Milazzo L, Mercanti D, Volonté C (2000) Antagonists of P2 receptor prevent NGF-dependent neuritogenesis in PC12 cells. Neuropharmacology 39:1083-1094.

Durham HD, Dahrouge S, Cashman NR (1993) Evaluation of the spinal cord neuron X neuroblastoma hybrid cell line NSC-34 as a model for neurotoxicity testing. Neurotoxicology 14:387-395.

Flobak Å, Skånland SS, Hovig E, Taskén K, Russnes HG (2022) Functional precision cancer medicine: drug sensitivity screening enabled by cell culture models. Trends Pharmacol Sci 43:973-985.

Foster LA, Salajegheh MK (2019) Motor neuron disease: pathophysiology, diagnosis, and management. Am J Med 132:32-37.

Garone MG, D'Antoni C, Rosa A (2022) Culture of human iPSC-derived motoneurons in compartmentalized microfluidic devices and quantitative assays for studying axonal phenotypes. Methods Mol Biol 2429:189-199.

Gökbuget N, Hoelzer D (2009) Treatment of adult acute lymphoblastic leukemia. Semin Hematol 46:64-75.

Imamura K, Kawaguchi J, Shu T, Inoue H (2021) Generation of motor neurons from human ESCs/iPSCs using sendai virus vectors. Methods Mol Biol 2352:127-132.

Liguori F, Amadio S, Volonté C (2021) Where and why modeling amyotrophic lateral sclerosis. Int J Mol Sci 22:3977.

Livak KJ, Schmittgen TD (2001) Analysis of relative gene expression data using real-time quantitative PCR and the 2(-Delta Delta C(T)) Method. Methods 25:402-408.

Maier O, Böhm J, Dahm M, Brück S, Beyer C, Johann S (2013) Differentiated NSC-34 motoneuron-like cells as experimental model for cholinergic neurodegeneration. Neurochem Int 62:1029-1038.

Marchioretti C, Andreotti R, Zuccaro E, Lieberman AP, Basso M, Pennuto M (2023) Spinal and bulbar muscular atrophy: From molecular pathogenesis to pharmacological intervention targeting skeletal muscle. Curr Opin Pharmacol 71:102394.

Martire A, Pepponi R, Liguori F, Volonté C, Popoli P (2020) P2X7 receptor agonist 2'(3')-O-(4-Benzoylbenzoyl)ATP differently modulates cell viability and corticostriatal synaptic transmission in experimental models of Huntington's disease. Front Pharmacol 11:633861.

Marzoughi S, Pfeffer G, Cashman N (2023) Primary lateral sclerosis. Handb Clin Neurol 196:89-99.

Matusica D, Fenech MP, Rogers ML, Rush RA (2008) Characterization and use of the NSC-34 cell line for study of neurotrophin receptor trafficking. J Neurosci Res 86:553-565.

Nango H, Kosuge Y, Miyagishi H, Sugawa K, Ito Y, Ishige K (2017) Prostaglandin E2 facilitates neurite outgrowth in a motor neuron-like cell line, NSC-34. J Pharmacol Sci 135:64-71.

Nango H, Kosuge Y, Sato M, Shibukawa Y, Aono Y, Saigusa T, Ito Y, Ishige K (2020) Highly efficient conversion of motor neuron-like NSC-34 Cells into functional motor neurons by prostaglandin E2. Cells 9:1741.

Nango H, Kosuge Y (2022) Present state and future perspectives of prostaglandins as a differentiation factor in motor neurons. Cell Mol Neurobiol 42:2097-2108.

Pérez V, Bermedo-Garcia F, Zelada D, Court FA, Pérez M, Fuenzalida M, Ábrigo J, Cabello-Verrugio C, Moya-Alvarado G, Tapia JC, Valenzuela V, Hetz C, Bronfman FC, Henríquez JP (2019) The p75NTR neurotrophin receptor is required to organize the mature neuromuscular synapse by regulating synaptic vesicle availability. Acta Neuropathol Commun 7:147.

Qin H, Zhao A, Ma K, Fu X (2018) Chemical conversion of human and mouse fibroblasts into motor neurons. Sci China Life Sci 61:1151-1167.

Ramya V, Sarkar N, Bhagat S, Pradhan RK, Varghese AM, Nalini A, Sathyaprabha TN, Raju TR, Vijayalakshmi K (2023) Oligodendroglia confer neuroprotection to NSC-34 motor neuronal cells against the toxic insults of cerebrospinal fluid from sporadic amyotrophic lateral sclerosis patients. Mol Neurobiol 60:4855-4871.

Scholzen T, Gerdes J (2000) The Ki-67 protein: from the known and the unknown. J Cell Physiol 182:311-322.

Sobecki M, et al. (2016) The cell proliferation antigen Ki-67 organises heterochromatin. Elife 5:e13722.

Stanzione A, Polini A, La Pesa V, Quattrini A, Romano A, Gigli G, Moroni L, Gervaso F (2021) Thermosensitive chitosan-based hydrogels supporting motor neuron-like NSC-34 cell differentiation. Biomater Sci 9:7492-7503.

Takagaki K, Katsuma S, Kaminishi Y, Horio T, Tanaka T, Ohgi T, Yano J (2005) Role of Chk1 and Chk2 in Ara-C-induced differentiation of human leukemia K562 cells. Genes Cells 10:97-106.

Takagi M, Nishiyama Y, Taguchi A, Imamoto N (2014) Ki67 antigen contributes to the timely accumulation of protein phosphatase 1γ on anaphase chromosomes. J Biol Chem 289:22877-22887.

Tsuchida T, Ensini M, Morton SB, Baldassare M, Edlund T, Jessell TM, Pfaff SL (1994) Topographic organization of embryonic motor neurons defined by expression of LIM homeobox genes. Cell 79:957-970.

Valetdinova KR, Medvedev SP, Zakian SM (2015) Model systems of motor neuron diseases as a platform for studying pathogenic mechanisms and searching for therapeutic agents. Acta Naturae 7:19-36.

Volonté C, Ciotti MT, Battistini L (1994) Development of a method for measuring cell number: application to CNS primary neuronal cultures. Cytometry 17:274-276.

Wiese S, Herrmann T, Drepper C, Jablonka S, Funk N, Klausmeyer A, Rogers ML, Rush R, Sendtner M (2010) Isolation and enrichment of embryonic mouse motoneurons from the lumbar spinal cord of individual mouse embryos. Nat Protoc 5:31-38.

Wu D, Khan FA, Zhang K, Pandupuspitasari NS, Negara W, Guan K, Sun F, Huang C (2024) Retinoic acid signaling in development and differentiation commitment and its regulatory topology. Chem Biol Interact 387:110773.

Zhao W, Beers DR, Thonhoff JR, Thome AD, Faridar A, Wang J, Wen S, Ornelas L, Sareen D, Goodridge HS, Svendsen CN, Appel SH (2020) Immunosuppressive functions of M2 macrophages derived from iPSCs of patients with ALS and healthy controls. iScience 23:101192.

C-Editor: Zhao M; S-Editor: Li CH; L-Editors: Li CH, Song LP; T-Editor: Jia Y